Global analysis with SNO: Toward the solution of the solar neutrino problem

P. I. Krastev
Philips Analytical, Natick, Massachusetts 01760

A. Yu. Smirnov
The Abdus Salam International Centre for Theoretical Physics, I-34100 Trieste, Italy
and Institute for Nuclear Research of Russian Academy of Sciences, Moscow 117312, Russia
(Received 15 November 2001; published 29 March 2002)

We perform a global analysis of the latest solar neutrino data including the Solar Neutrino Observatory (SNO) result on the charged current (CC) event rate. This result further favors the large mixing angle (LMA) Mikheyev-Smirnov-Wolfenstein (MSW) solution of the solar neutrino problem. The best fit values of parameters we find are $\Delta m^2=(4.8–5.0)\times 10^{-5}$ eV^2, $\tan^2\theta=0.35–0.38$, $f_{\rm B}=1.08–1.12$, and $f_{\rm hep}=1–4$, where $f_{\rm B}$ and $f_{\rm hep}$ are the boron and $^3{\rm He}+p$ (hep) neutrino fluxes in units of the corresponding fluxes in the standard solar model (SSM). With respect to this best fit point the low Δm^2 (LOW) MSW solution is accepted at 90% C.L. The vacuum oscillation solution (VAC) with $\Delta m^2=1.4\times 10^{-10}$ eV^2, gives a good fit to the data provided that the boron neutrino flux is substantially smaller than the SSM flux ($f_{\rm B}\sim 0.5$). The small mixing angle (SMA) solution is accepted at about the 3σ level. We find that vacuum oscillations to a sterile neutrino, VAC(sterile), with $f_{\rm B}\sim 0.5$ also give a rather good global fit to the data. All other sterile neutrino solutions are strongly disfavored. We check the quality of the fit by constructing the pull-off diagrams of observables for the global solutions. Maximal mixing is allowed at the 3σ level in the LMA region and at 95% C.L. in the LOW region. Predictions for the day-night asymmetry, spectrum distortion, and ratio of the neutral to charged current event rates [NC]/[CC] at SNO are calculated. In the best fit points of the global solutions we find $A_{DN}^{CC}\approx 7–8\,\%$ for the LMA, $\sim 3\%$ for the LOW, and $2-3\%$ for the SMA regions. In the LMA region the asymmetry can be as large as $15–20\%$. Observation of $A_{DN}^{CC}>5\%$ will further favor the LMA solution. It will be difficult to see the distortion of the spectrum expected for LMA as well as LOW solutions. However, future SNO spectral data can significantly affect the VAC and SMA solutions. We present the expected values of the BOREXINO event rate for global solutions.

DOI: 10.1103/PhysRevD.65.073022 PACS number(s): 14.60.Lm, 14.60.Pq, 26.65.+t, 95.85.Ry

I. INTRODUCTION

With the Solar Neutrino Observatory (SNO) result [1,2] on the charged current (CC) rate, we now, for the first time ever, have more than 3σ evidence of flavor conversion of solar neutrinos. ''Smoking guns'' have indeed started to smoke. The statement, made first in the original publication by the SNO Collaboration, is based on the difference of the boron neutrino fluxes determined from the CC event rate in the SNO detector, and the νe scattering event rate obtained by the SuperKamiokande (SK) [3] Collaboration (and confirmed, albeit with smaller statistical significance, by SNO). Somewhat paradoxically, the absence of a significant distortion of the boron neutrino spectrum at SuperKamiokande adds to the strength of this conclusion.

In general, the difference between the signals in the SNO and SK detectors can be due to (1) the appearance of the ν_μ,ν_τ flux, or/and (2) the distortion of the neutrino energy spectrum. If the suppression of the boron neutrino flux (due to some neutrino transformations) increases with increasing neutrino energy, then the higher sensitivity to higher energies of the CC reaction in SNO as compared with νe scattering in SK would explain the lower rate in SNO.

In fact, both reasons imply neutrino conversion. However, the absence of a strong distortion of the boron neutrino spectrum, as found by SuperKamiokande and independently confirmed by SNO, leads to the conclusion that the main reason for the difference is the appearance of the ν_μ,ν_τ flux.

From the SNO result and its comparison with the SK data one can immediately draw several conclusions: A strong deficit of the ν_e flux with respect to the standard solar model (SSM) predictions is found; there is strong evidence that ν_e's from the Sun are converted to ν_μ,ν_τ; there is no astrophysical solution of the solar neutrino problem (for a recent quantitative analysis see [4]); solutions of the solar neutrino problem based on pure active-sterile conversion $\nu_e\to\nu_s$ are strongly disfavored; and more than half of the original ν_e flux is transformed to neutrinos of a different type, ν_μ, ν_τ, and possibly ν_s, that is, the ν_e survival probability

$$P<1/2. \tag{1}$$

In fact, with the assumption of a pure active transition one gets $P=0.334\pm 0.22$ [2], which is just $\sim 1\sigma$ below 1/2. Clearly, if the sterile neutrino component is present in the flux, the survival probability is even smaller. The inequality (1), if confirmed, will have crucial implications for further experimental developments in the field, as well as for fundamental theory.

We know now with high confidence that electron neutrinos produced in the center of the Sun undergo flavor conversion. However the specific mechanism of the conversion has not yet been identified. As we will see, only some extreme

possibilities are excluded by adding the SNO result to the previously available solar neutrino data. A number of solutions still exist.

The SNO result changes the status of specific solutions to the solar neutrino problem. The changes can be immediately seen by comparing predictions for the CC event rate from global solutions found in the pre-SNO analysis [5,6] with the SNO result. There are four solutions, three active and one sterile, which give predictions close to the SNO result:

$$R_{CC}^{SNO} \equiv \frac{\text{SNO}}{\text{SSM}} = 0.347 \pm 0.029. \quad (2)$$

(1) The large mixing angle (LMA) Mikheyev-Smirnov-Wolfenstein (MSW) solution: the 3σ prediction interval $R_{CC}=0.20$–0.41 covers the SNO result ($R_{CC} \equiv$[CC] from [5]). The best fit point from the pre-SNO analysis, $R_{CC}=0.31$, is slightly ($\sim 1\sigma$) below the central value given by SNO. Therefore, the SNO result shifts the region of the LMA solution and the best fit point to larger values of mixing angles, which correspond to larger survival probability.

(2) The low Δm^2 (LOW) solution: the interval of predictions $R_{CC}=0.36$–0.42 is above the SNO result. In the best fit point R_{CC} is 2σ (experimental) higher than the central SNO value. Therefore this solution is somewhat less favored, and the SNO result tends to shift the allowed region to smaller values of θ, which correspond to smaller survival probability.

(3) The vacuum oscillation (VAC) solution: the expected interval $R_{CC}=0.33$–0.42 also covers the SNO range, and the best fit value $R_{CC}=0.38$ is just 1σ above the central SNO result. Therefore, the SNO result improves the status of this solution.

(4) The solution of vacuum oscillations to sterile neutrinos, VAC(sterile): the predicted interval $R_{CC}=0.36$–0.41, with the best fit point 0.39, is only slightly higher than for the VAC(active) case. Here the low rate predicted for SNO is due to the difference of the thresholds in the SNO and SK experiments and to the steep increase of the suppression with neutrino energy. This solution survives the first SNO result.

Other solutions look less favorable in the light of the SNO result. In particular, the small mixing angle (SMA) MSW solution interval $R_{CC}=0.37$–0.50 (especially its best fit point 0.46 from the pre-SNO analysis) is substantially above the SNO rate. This solution is further disfavored by the SNO result. In fact, the SMA solution predicts the opposite energy dependence of the suppression on the neutrino energy to the one SNO prefers.

The just-so^2(active), SMA(sterile) and just-so^2(sterile) solutions predict essentially the same rate for the SK and SNO experiments and therefore are strongly disfavored.

The statements above are supported by a detailed quantitative analysis of the solar neutrino data that we have performed in this paper. The results of this analysis are described in the rest of this paper. Previously some of the same conclusions were reported in [7–10]; see also the related studies [11–14].

The paper is organized as follows. In Sec. II we present the results of the global analysis of the solar neutrino data. We construct the pull-off diagrams of available observables for the global solutions found. In Sec. III we consider the specifics of the global solutions and their implications. We evaluate the quality of the data fit in each of the global solutions. We calculate predictions for the day-night asymmetry and spectrum distortion in Sec. IV. Finally, prospects for identifying the solution to the solar neutrino problem are discussed in Sec. V.

II. GLOBAL ANALYSIS AND PULL-OFF DIAGRAMS

We describe here the results of a global analysis of the solar neutrino data. We find global solutions (sets of oscillation parameters and solar neutrino fluxes that explain the solar neutrino data) and determine the goodness of fit (g.o.f.) of the best fit points. We perform diagnostics of the global solutions by checking their stability with respect to variations in the analysis and to uncertainties in the original solar neutrino fluxes. To check the quality of the fit we construct the pull-off diagrams for the observables.

A. Features of the analysis

We follow the procedure of the analysis developed in our previous publications [15–17,5] in collaboration with Bahcall. We also describe some additional features, which should be taken into account when comparing our results with those obtained by other groups.

In our global analysis we use (i) the Ar-production rate from the Homestake experiment [18], (ii) the Ge-production rate from SAGE [19], (iii) the combined Ge-production rate from GALLEX and GNO [20,21], (iv) the CC event rate measured by SNO [1], and (v) the day and night energy spectra measured by SuperKamiokande [3].

Following the procedure outlined in [5] we do not include the total rate of events in the SK detector, which is not independent of the spectral data. In our standard global analysis, we use 4 rates and 38 spectral data, a total of 42 data points. The number of free parameters and the number of degrees of freedom (d.o.f.) are different in different analyses and we will specify them later.

The solar neutrino fluxes are taken according to the Bahcall-Pinsonneault 2000 (BP2000) SSM [22] with the corrected (due to improved measurement of the solar luminosity) boron neutrino flux $F_{\rm B}^{SSM}=5.05\times 10^6$ cm$^{-2}\,c^{-1}$. We denote by $f_{\rm B}$ and $f_{\rm hep}$ the fluxes of the boron and $^3{\rm He}+p$ (hep) neutrinos measured in units of the BP2000 fluxes.

The analysis of the data is performed in terms of two-neutrino mixing characterized by the mass squared difference Δm^2 and the mixing parameter $\tan^2\theta$. We consider conversion into pure active or pure sterile neutrinos.

We perform the χ^2 test of various oscillation solutions by calculating

$$\chi^2_{global} = \chi^2_{rate} + \chi^2_{spectrum}, \quad (3)$$

where χ^2_{rate} and $\chi^2_{spectrum}$ are the contributions from the total rates and from the SuperKamiokande day and night spectra, respectively. Each of the entries in Eq. (3) is a function of the

TABLE I. Best fit values of the parameters Δm^2, $\tan^2\theta$, f_B, and f_{hep} from the free flux analysis. The minimum χ^2 and the corresponding g.o.f. are given in the last two columns. The number of degrees of freedom is 38: 4 rates (Homestake, SAGE, GALLEX/GNO, SNO) + 38 SK spectra points − 4 parameters.

Solution	Δm^2 (eV^2)	$\tan^2\theta$	f_B	f_{hep}	χ^2_{min}	g.o.f.
LMA	4.8×10^{-5}	0.35	1.12	4	29.2	0.85
VAC	1.4×10^{-10}	0.40 (2.5)	0.53	6	32	0.74
LOW	1.1×10^{-7}	0.66	0.88	2	34.3	0.64
SMA	6.0×10^{-6}	1.9×10^{-3}	1.12	4	40.9	0.34
Just-So^2	5.5×10^{-12}	1.0	0.44	0	45.8	0.18
VAC(sterile)	1.4×10^{-10}	0.38 (2.6)	0.54	9	35.1	0.60
Just-So^2(sterile)	5.5×10^{-12}	1.0	0.44	0	46.2	0.17
SMA(sterile)	3.8×10^{-6}	4.2×10^{-4}	0.52	0.2	48.2	0.12
LMA(sterile)	1.0×10^{-4}	0.33	1.14	0	49.0	0.11
LOW(sterile)	2.0×10^{-8}	1.05	0.83	0	49.2	0.11

four parameters (Δm^2, $\tan^2\theta$, f_B, and f_{hep}). It is an important feature of our approach [5] that at each step of the minimization process these parameters are kept the same in each of the two entries on the right-hand side of Eq. (3).

B. Free flux fit

We perform the fit to the experimental data treating the boron neutrino flux f_B, and the hep neutrino flux f_{hep}, as free parameters. There are several reasons to consider f_B and f_{hep} as free parameters (for earlier work in this context see [23]).

(1) These fluxes have the largest uncertainties in the SSM (see, however, [24]).

(2) The goal of the solar neutrino studies is to find directly from the solar neutrino data both the oscillation parameters and the neutrino fluxes. The free flux analysis is a way to achieve this goal.

(3) Comparing the fluxes f_{hep} and f_B found from the free flux analysis with the SSM fluxes we can estimate the plausibility of the fit and the reliability of the solutions. Clearly, strong deviation of the fluxes for a given solution from the SSM values will indicate certain problems with either the solution or the SSM predictions.

(4) Last, but not least, this fit is the most conservative one regarding the exclusion of certain scenarios.

Thus, together with Δm^2 and $\tan^2\theta$, there are four free parameters and therefore $42-4=38$ d.o.f. in the χ^2 fit. In Table I we show the best fit values of the parameters Δm^2, $\tan^2\theta$, f_B, and f_{hep} for different solutions of the solar neutrino problem. We also give the corresponding values of χ^2_{min} and the goodness of the fit. Several remarks are in order.

The absolute χ^2 minimum, $\chi^2=29.2$, is in the LMA region. Such a low χ^2 for 38 d.o.f. is mainly due to the small spread of the experimental points in both the day and the night SK spectra. A similar situation is realized for the LOW solution. The SuperKamiokande day and night spectra can be especially well described by solutions that predict a bump in the survival probability at $E=6-8$ MeV and a dip at $E=10-11$ MeV. This is the case of VAC solutions (both active and sterile) with large hep flux. It is for this reason that VAC solutions have high goodness of the global fit. According to Table I the VAC(sterile) solution is in the fourth position after the LMA, VAC(active), and LOW solutions, its fit being only slightly worse than that of the LOW solution. The VAC(sterile) solution has, however, a number of problems which we will discuss in the next section.

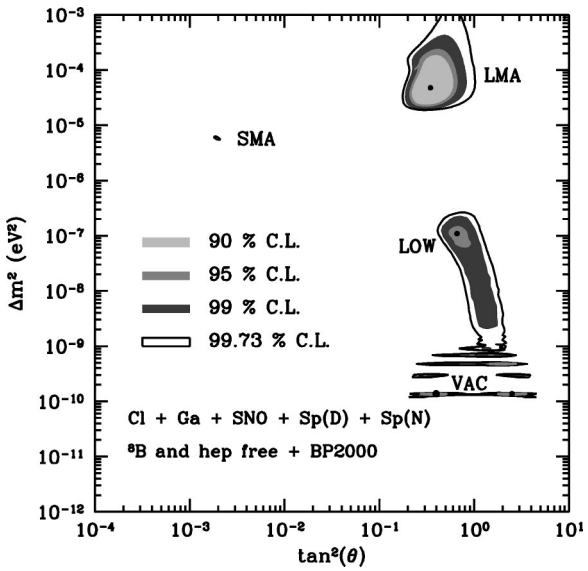

FIG. 1. Global solutions from free flux analysis. The boron and hep neutrino fluxes are considered as free parameters. The best fit points are marked by dark circles. The absolute minimum of the χ^2 is in the LMA region. The allowed regions are shown at 90%,95%,99%, and 99.73% C.L.'s with respect to the global minimum in the LMA region.

For LMA, LOW, and SMA solutions values of f_B, agree with the SSM predictions within 1σ theoretical uncertainty ($\sim$18%). All VAC solutions and SMA(sterile), as well as just-so^2 solutions, appear with a boron flux that is 3σ below the SSM boron neutrino flux. For the hep neutrino flux the LMA, VAC, and SMA solutions imply significant (factors of 4–6) deviation from the central SSM value. However, a hep flux consistent with the SSM is still acceptable and does not significantly alter the goodness of fit (see the next section). The VAC(sterile) solution requires even larger hep neutrino flux, namely, about nine times larger than the SSM value.

For VAC solutions the matter effect is negligible and in the Table I two ''symmetric'' values of $\tan^2\theta$, $\tan^2\theta_1 = 1/\tan^2\theta_2$, correspond to mixing in the normal and dark (in parentheses) sides of the parameter space.

Even within this conservative analysis the LMA(sterile) and LOW(sterile) solutions give a very bad fit and in what follows we will not discuss them. Just-so^2 (active) and just-so^2 (sterile) give very similar descriptions of the data so we will present results for only one of them.

In Fig. 1 we show contours of constant (90,95,99,99.73%) confidence level with respect to the absolute minimum in the LMA region. Following the same procedure as in [5] the contours have been constructed in the following way. For each point in the Δm^2,$\tan^2\theta$ plane we

TABLE II. Best fit values of the parameters Δm^2, $\tan^2\theta$, and f_B from the global analysis with $f_{hep}=1$. The minimum χ^2 and the corresponding g.o.f. are given in the last two columns. The number of degrees of freedom is 38: 4 rates (Homestake, SAGE, GALLEX/GNO, SNO) + 38 SK spectral points − 4 parameters.

Solution	Δm^2 (eV^2)	$\tan^2\theta$	f_B	χ^2_{min}	g.o.f.
LMA	5.0×10^{-5}	0.36	1.1	30.1	0.85
VAC	1.4×10^{-10}	0.363 (2.7)	0.54	33.4	0.72
LOW	1.1×10^{-7}	0.69	0.86	34.5	0.67
SMA	5.5×10^{-6}	1.9×10^{-3}	1.04	42.2	0.33
Just-So^2	5.5×10^{-12}	1.0	0.44	46.4	0.19
VAC(sterile)	1.4×10^{-10}	0.35 (2.9)	0.55	36.9	0.57
SMA(sterile)	3.8×10^{-6}	4.2×10^{-4}	0.52	48.6	0.14

find the minimal value $\chi^2_{min}(\Delta m^2,\tan^2\theta)$ the varying f_B and f_{hep}. We define the contours of constant confidence level by the condition

$$\chi^2_{min}(\Delta m^2,\tan^2\theta)=\chi^2_{min}(\mathrm{LMA})+\Delta\chi^2, \tag{4}$$

where $\chi^2_{min}(\mathrm{LMA})=29.3$ is the absolute minimum in the LMA region and $\Delta\chi^2$ is taken for two degrees of freedom.

To clarify the role of the hep neutrino flux we present in Table II the result of the χ^2 analysis when $f_{hep}=1$, treating only f_B as a free parameter. It follows from Table II that fixing the flux f_{hep} leads to a rather small change of the oscillation parameters. At the same time, the constraint $f_{hep}=1$ lowers the goodness of fit of solutions that imply a large value of f_{hep} in the free flux analysis. We get $\Delta\chi^2=1.8$ for VAC(sterile), $\Delta\chi^2=1.4$ for SMA, and $\Delta\chi^2=1.4$ for VAC(active) solutions.

According to Ref. [24] the calculated hep neutrino flux has about 20% uncertainty. Therefore solutions that require large f_{hep} (2–9) are disfavored and the results of the fit with $f_{hep}=1$ look more relevant.

C. SSM restricted global fit

In order to check the significance of the SSM restriction on the boron neutrino flux we have performed the fit to the data adding to the χ^2 sum in Eq. (3) the term

$$\left(\frac{f_B-1}{\sigma_B}\right)^2, \tag{5}$$

where $\sigma_B=0.18$ is the average (of the upper and lower) 1σ theoretical error of the flux in the BP2000 model [22]. With the term (5) included in our global χ^2 we, in a way, treat the SSM prediction for the boron neutrino flux as an independent ''measurement'' and consider it as an additional degree of freedom. This procedure makes sense because a significant contribution to the error in the SSM determination of the boron neutrino flux comes from the *measurements* of the p-Be cross section.

One ''technical'' remark is in order. Our approach differs from analyses where the boron neutrino flux is taken as a theoretical prediction from the SSM [8,9]. In the latter case the term (5) is absent, the central SSM value is used in the predictions of observables, and the theoretical errors on the boron neutrino flux are added to the experimental errors.

TABLE III. Best fit values of the parameters Δm^2, $\tan^2\theta$, f_B, and f_{hep} from the SSM restricted global analysis. f_{hep} is considered as a free parameter. The minimum χ^2 and the corresponding g.o.f. are given in the last two columns. The number of degrees of freedom is 40: 4 rates (Homestake, SAGE, GALLEX/GNO, SNO) +38 SK spectral points +1 (f_B) −3 parameters.

Solution	Δm^2 (eV^2)	$\tan^2\theta$	f_B	f_{hep}	χ^2_{min}	g.o.f.
LMA	5.0×10^{-5}	0.36	1.10	4.0	29.5	0.84
SMA	5.5×10^{-6}	1.9×10^{-3}	1.10	4.0	41.2	0.33
LOW	1.1×10^{-7}	0.66	0.88	2.0	34.7	0.62
VAC	4.8×10^{-10}	1.9	0.72	0.0	35.4	0.59
Just-So^2	5.5×10^{-12}	1.4	0.44	1.0	55.4	0.03
VAC(sterile)	1.4×10^{-10}	2.63	0.55	8.0	41.3	0.33
SMA(sterile)	4.0×10^{-6}	4.8×10^{-4}	0.54	2.0	54.5	0.04

In Table III and Fig. 2 we present the results of the fit with the SSM constrained boron neutrino flux. As expected, the most significant changes in comparison with the free flux analysis (Table I) appear in those solutions and regions of the oscillation parameters which imply strong deviation of f_B from 1. Our results show that mostly the best fit points as well as the χ^2_{min} and goodness of fit of the VAC(active), just-so^2, VAC(sterile), and SMA(sterile) solutions are affected. Thus, for the VAC(active) solution $\Delta\chi^2_{min}=3.4$, and for VAC(sterile) $\Delta\chi^2_{min}=6.2$. Moreover, the best fit VAC solution shifts to another point of the oscillation parameters in agreement with results of other groups. There is no signifi-

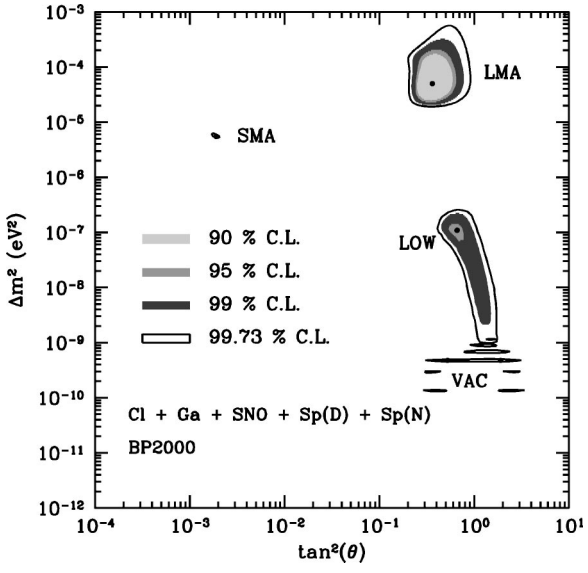

FIG. 2. Global solutions for the SSM restricted boron neutrino flux. hep neutrino flux is free. The best fit points are marked by dark circles. The absolute minimum of the χ^2 is in the LMA region. The allowed regions are shown at 90%,95%,99%, and 99.73% C.L.'s with respect to the global minimum in the LMA region.

TABLE IV. Best fit values of the parameters Δm^2 and $\tan^2\theta$ from the ''rates only'' analysis. The minimum χ^2 and the corresponding g.o.f. are given in the last two columns. The number of degrees of freedom is 3: 5 rates (Homestake, SAGE, GALLEX/GNO, SNO, SK) -2 parameters.

Solution	Δm^2 (eV^2)	$\tan^2\theta$	χ^2_{min}	g.o.f.
LMA	2.9×10^{-5}	0.36	3.55	0.31
SMA	7.9×10^{-6}	1.4×10^{-3}	5.1	0.16
LOW	1.0×10^{-7}	0.66	7.9	0.05
VAC	7.9×10^{-11}	3.5	2.24	0.52
Just-So^2	5.5×10^{-12}	2.0	16.4	0.0009
SMA(sterile)	4.4×10^{-6}	1.0×10^{-3}	17.4	0.0006
VAC(sterile)	1.0×10^{-10}	0.35	6.4	0.094

cant change of the LMA, LOW, and SMA best fit points and goodness of fit.

In Fig. 2 we show the contours of constant (90,95,99,99.73 %) confidence level for two degrees of freedom with respect to the absolute minimum in the LMA region.

D. Analysis of "rates only"

To clarify the relative significance of the total rates and the SK spectrum in the global analysis of the data we have performed a fit to the rates in the five experiments Homestake, SAGE, GALLEX/GNO, SNO, and SK. In this analysis we use the total rate of events in SK but do not use the SK energy spectrum of the recoil electrons. The results of the χ^2 test are summarized in Table IV.

Notice that with the SNO result the SMA solution no longer gives the best fit to the ''rates only,'' in contrast with pre-SNO analyses. The best fit is obtained in the VAC solution region. However, the parameters of this solution differ significantly from the parameters of the global solution when spectral data are included.

The ''rates only'' fit shifts the LMA region to smaller Δm^2. The LOW solution is essentially unchanged. Now VAC(sterile) and LOW have low goodness of fit.

Notice that in the absence of the spectral data the value of χ^2_{min} is comparable to or larger than the number of d.o.f.

E. Pull-off diagrams

In order to check the quality of the fits we have calculated predictions for the available observables at the best fit points of the global solutions found in the free flux analysis (see Table V). Using these predictions we have constructed the ''pull-off'' diagrams (Fig. 3) which show the deviations D_K of the predicted values of observables K from the central experimental values expressed in units of 1σ:

$$D_K \equiv \frac{K_{bf}-K_{expt}}{\sigma_K}, \qquad K \equiv Q_{\rm Ar}, Q_{\rm Ge}, R_{CC}, R_{\nu e}, A_{DN}^{SK}. \tag{6}$$

Here σ_K is the 1σ standard deviation for a given observable K. We take the experimental errors only: $\sigma_K = \sigma_K^{expt}$. The theoretical errors are related mainly to the uncertainty in the boron neutrino flux. Since $f_{\rm B}$ is treated as a free parameter we do not take into account its theoretical errors. The remaining theoretical errors are small and strongly correlated in $Q_{\rm Ar}$, R_{CC}, and $R_{\nu e}$.

TABLE V. Values of the total rates in Cl, Ga, SK, and SNO experiments at the best fit points of global solutions found in the free flux analysis. The rates in the radiochemical experiments are given in solar neutrino units. For SuperKamiokande and SNO the ratios of the best fit rates to the rates predicted in the SSM are given.

Solution	Cl	Ga	SK	SNO
LMA	2.89	71.3	0.452	0.323
SMA	2.26	74.4	0.463	0.396
LOW	3.12	68.5	0.446	0.368
VAC	3.13	70.2	0.423	0.364
Just-So^2	3.00	70.8	0.434	0.434
SMA(sterile)	2.93	75.5	0.435	0.445
VAC(sterile)	3.24	69.9	0.414	0.381
Just-So^2	3.01	70.9	0.434	0.435

The diagrams are good diagnostics of the fit. They allow

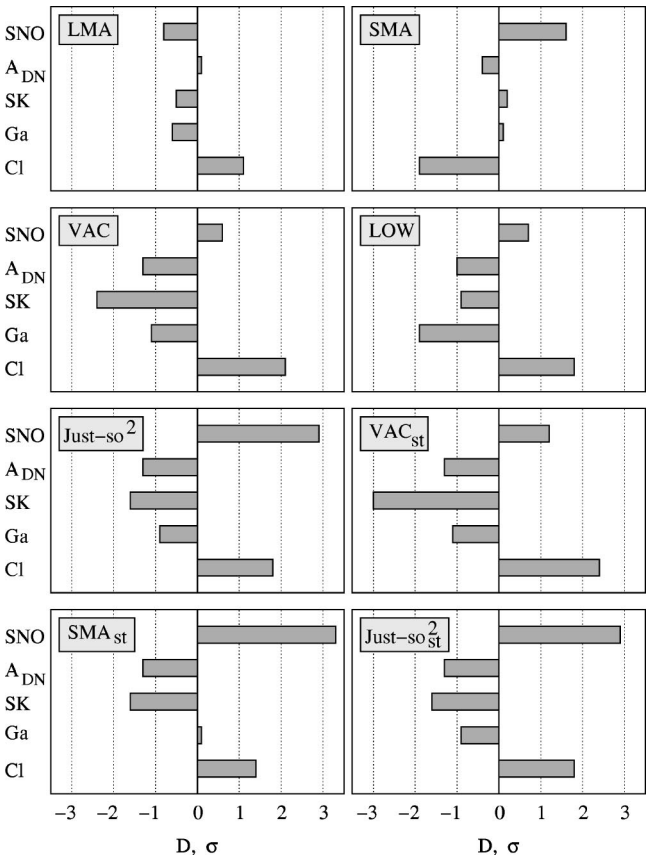

FIG. 3. Pull-off diagrams for global solutions. Shown are deviations of predictions for the Ar-production rate, Ge-production rate, SK rate, day-night asymmetry at SK, and SNO rate from experimentally measured values. The pull-offs are expressed in units of one standard deviation, 1σ.

one to pin down problems that some of the solutions have and to elaborate criteria for further checks.

According to Fig. 3 only the LMA solution does not have strong deviations of the predictions from the experimental results. The LOW, VAC, and SMA solutions give somewhat worse fits to the data. The fit from other solutions is very bad.

The pull-off diagrams give some clarification to a common concern, namely, that the high statistics SK experiment (in particular its spectral data) overwhelms the rate data in the global analysis. In particular, solutions, that are strongly disfavored by the rates give a good fit when spectral data are included.

This problem can be approached in a different way: one can use just one parameter, e.g., the first moment, which describes possible distortions of the recoil electron energy spectrum [25].

III. GLOBAL SOLUTIONS: PROPERTIES AND IMPLICATIONS

Here we evaluate the status of global solutions using the following criteria: (1) goodness of the global fit in the free flux analysis; (2) deviation of the boron and hep neutrino fluxes found in the free flux analysis from the SSM value fluxes, that is, the deviation of $f_{\rm B}$ and $f_{\rm hep}$ from 1; (3) goodness of the fit in the SSM restricted analysis and in the ''rates only'' analysis; (4) stability of the solution with respect to variations of the analysis; and (5) quality of the fit of the individual observables, i.e., features of the pull-off diagram; a deviation by more than 3σ for some observables is a clear signal of trouble. We identify solutions that pass all of these criteria.

A. The best fit solution: LMA

The SNO result further favors the LMA solution [26]. In all global analyses in which the SK spectral data are included, the LMA method gives the minimal χ^2. The best fit point from the free flux analysis is

$$\Delta m^2 = 4.8\times 10^{-5}\ \text{eV}^2, \qquad \tan^2\theta = 0.35,$$

$$f_{\rm B} = 1.2, \qquad f_{\rm hep} = 4.0. \tag{7}$$

A large $f_{\rm hep}$ is needed to account for some excess of the SK events in the high energy part of the spectrum. For $f_{\rm hep}=1$, values of the oscillation parameters are practically the same as in the free flux analysis (see Table II), and the goodness of the fit is even slightly higher. The boron neutrino flux is 20% higher than the central value in the SSM: $F_{\rm B}=f_{\rm B}\times F_{\rm B}^{SSM}=5.66\times 10^{6}\ \text{cm}^{-2}\,c^{-1}$ being, however, within 1σ deviation. This flux is rather close to the central value extracted from the SNO and SK data [1].

The fit of the data with the SSM restricted $f_{\rm B}$ gives a minimum of χ^2 at essentially the same values of parameters as in Eq. (7).

The values of the oscillation parameters (7) found here are very close to the values found by other groups [8,9]. This shows that the solution is robust and does not change with the type of analysis.

Notice that the SNO data lead to a shift of the best fit point (as well as the whole region) to larger values of $\tan^2\theta$ as was discussed in the Introduction.

According to the pull-off diagram, the LMA solution reproduces observables at $\sim 1\sigma$ or better. The largest deviation is for the Ar-production rate: the solution predicts a 1.1σ larger rate than the Homestake result.

The ''rates only'' analysis shifts the best fit point to smaller Δm^2.

Considering the allowed regions at different confidence levels we find the following.

(1) Δm^2 is rather sharply restricted from below by the day-night asymmetry of the SK event rate: $\Delta m^2 > 2\times 10^{-5}\ \text{eV}^2$ at 99.73% C.L.

(2) The upper bound on Δm^2 is of great importance for future experiments, in particular for the neutrino factories [27]. We find, from the free flux fit (the CHOOZ bound is not included),

$$\Delta m^2 \leqslant \begin{cases} 1.9\times 10^{-4}\ \text{eV}^2, & 90\%\ \text{C.L.}, \\ 2.3\times 10^{-4}\ \text{eV}^2, & 95\%\ \text{C.L.}, \\ 4.3\times 10^{-4}\ \text{eV}^2, & 99\%\ \text{C.L..} \end{cases} \tag{8}$$

Similar results can be obtained from the analysis in Ref. [8] where the CHOOZ data [28] have also been taken into account. The CHOOZ bound becomes important for larger values than $\Delta m^2 \sim 8\times 10^{-4}\ \text{eV}^2$ where it modifies the 3σ contour.

The fit with the SSM restricted f_B gives a stronger bound on Δm^2. Instead of the limits in Eq. (8), we get the upper bounds 1.7×10^{-4}, 2.1×10^{-4}, and $3.1\times 10^{-4}\ \text{eV}^2$ for 90%, 95%, and 99% C.L.'s respectively.

(3) The SNO and SK results (evidence of ν_μ, ν_τ appearance) give an important *lower* limit on mixing:

$$\tan^2\theta > 0.2, \qquad 99\%\ \text{C.L.} \tag{9}$$

(4) Maximal mixing is allowed only at the $\sim 3\sigma$ level:

$$\tan^2\theta \geqslant 1 \qquad \text{for} \quad \Delta m^2 = (4\text{–}10)\times 10^{-5}\ \text{eV}^2,$$

$$99.73\%\ \ \text{C.L.} \tag{10}$$

In spite of the shift of the best fit point to larger values of Δm^2 the C.L. for acceptance of maximal mixing is not lower than it was before the SNO result. The reason is that the SNO rate corresponds to a survival probability smaller than 1/2, which disfavors maximal mixing.

A similar result follows from the analysis in Ref. [8], where it was found that maximal mixing (at the 3σ level) is allowed for $\Delta m^2 = (4\text{–}20)\times 10^{-5}\ \text{eV}^2$.

In the fit with the SSM restricted $f_{\rm B}$, maximal mixing is even more disfavored: $\tan^2\theta < 0.9$ at the 99.73% C.L.

B. Large or small? The fate of the SMA solution

The fate of the SMA solution, the only solution that is based on small mixing, is of great importance for future developments in both theory and experiment.

We find that the SMA solution is only marginally allowed at the 3σ level (with respect to the global minimum) in the free flux fit. The best fit point parameters are

$$\Delta m^2 = 6.0\times 10^{-6}\ \text{eV}^2, \qquad \tan^2\theta = 0.0019,$$

$$f_{\rm B} = 1.12, \qquad f_{\rm hep} = 4. \tag{11}$$

The SNO result shifts the local minimum to substantially larger mixing angles in comparison with the pre-SNO result. This is a consequence of the appearance of the ν_μ/ν_τ flux, which implies large transition probability and therefore large mixing angles. At such a large $\tan^2\theta$ one expects significant distortion of the boron neutrino spectrum (see Sec. IV).

An important feature of the solution is a large flux of hep neutrinos. It is this large flux which, together with the correlated systematic error and $f_{\rm B}>1$, makes it possible to get a reasonable description of the SK energy spectrum. If the SSM value is taken for the hep neutrino flux (see Table II) the χ^2 increases by $\Delta\chi^2 = 1.4$.

These results are in agreement with those obtained in [8]. In [9], the SMA is accepted at lower than the 99% level. Surprisingly, in this analysis the SNO result shifts the mixing to even smaller values: the best fit value from [9] is at $\tan^2\theta = 4\times 10^{-4}$.

Before the SNO result, the SMA solution always gave the best fit to the total rates. Inclusion of the CC event rate measured by SNO moves the SMA solution to third position, after the VAC and LMA solutions. Furthermore, the fit is no longer good: $\chi^2_{min} = 5.1$ for three d.o.f. From the pull-off diagram we find that there is a tension between the SNO and Homestake rates: The SNO data (CC rate) require rather small survival probability for boron electron neutrinos. Furthermore, the gallium experiments imply strong suppression of the beryllium neutrino flux. This leads to a low (1.9σ) Ar-production rate. At the same time, according to Fig. 3 the CC event rate is 1.7σ higher than the SNO result.

For a mixing angle corresponding to the best fit point (11) one expects a significant regeneration effect in the core night bin [29] due to parametric enhancement of oscillations for the core crossing trajectories [30]. However, the day and night spectra we used in our analysis are not sensitive to this feature. The zenith angle distribution of events measured by the SK experiment does not show any core enhancement [3]. Inclusion of this information in the global analysis will further disfavor the SMA solution.

C. LOW solution: Next best?

For the best fit point of the free flux analysis we get

$$\Delta m^2 = 1.1\times 10^{-7}\ \text{eV}^2, \qquad \tan^2\theta = 0.66,$$

$$f_{\rm B} = 0.88, \qquad f_{\rm hep} = 2.0. \tag{12}$$

If the hep neutrino flux is fixed at its SSM value, $f_{\rm hep}=1$, the best fit point shifts to larger mixing: $\tan^2\theta = 0.69$. Notice that the solution implies $\sim 1\sigma$ lower boron neutrino flux than in the SSM.

In the analysis with the SSM restricted $f_{\rm B}$ the best fit point is the same as in Eq. (12).

The LOW solution gives a rather poor fit of the total rates, $\chi^2 = 7.9$ for 3 d.o.f. (see Table IV). In the best fit point we get 2σ larger Ar-production rate and 1.9σ lower Ge-production rate. It is this case where the overwhelming spectral information ''hides'' some problems with total rates in the global fit. The use of a single parameter for description of the spectrum distortion gives a much lower goodness of fit for the LOW solution as compared with the LMA solution [25].

D. VAC oscillation solution is back?

As anticipated from the comparison of the pre-SNO predictions with the SNO result the VAC solution improves its status. Indeed, at the best fit point of the free flux analysis,

$$\Delta m^2 = 1.4\times 10^{-10}\ \text{eV}^2, \qquad \tan^2\theta = 0.40\ \ (2.5),$$

$$f_{\rm B} = 0.53, \qquad f_{\rm hep} = 6.0, \tag{13}$$

the χ^2 is even lower than in the LOW solution. The solution with the parameters (13) was found in the pre-SNO analysis [5], but before the SNO result the goodness of the fit was substantially lower in comparison with those of other solutions.

The solution gives a very good description of the SK energy spectrum. The χ^2 is substantially smaller than the number of degrees of freedom. The solution reproduces rather precisely the bump in both the night and the day spectra at 7–8 MeV and the dip at 11–12 MeV. (These features can be well seen in Fig. 4e of Ref. [31].) The bump in the spectrum originates from the first maximum of the oscillation probability, which corresponds to the oscillation phase 2π. Above the bump the probability decreases with increasing energy and the increase of $R_{\nu e}$ at $E>12$ MeV is due to the large flux of the hep neutrinos.

Notice that an excellent description of the spectrum requires nonmaximal mixing, otherwise the distortion is very strong. The value of $\sin^2 2\theta$, which immediately determines the depth of oscillations, should be about 0.8. Then to compensate for the rather large survival probability and to explain the SNO result one needs to assume a small ($f_{\rm B}\sim 0.5$) original boron neutrino flux.

However, there are several problems with this solution. It requires substantially ($\sim 3\sigma$) lower original boron neutrino flux than in the SSM and substantially higher original hep neutrino flux: $f_{\rm hep}=6$. In the fit with $f_{\rm hep}=1$ the χ^2 increases by $\Delta\chi^2 = 1.4$.

For this solution one predicts seasonal asymmetry due to oscillations $A\approx -0.6A_0$, where $A_0\sim 7\%$ is the asymmetry due to the geometrical factor only ($1/R^2$ change of the flux). Thus one expects a suppressed seasonal asymmetry, in contrast with observations.

The solution gives a rather good fit to the rates, although in the ''rates only'' analysis the best fit point shifts to a different island in parameter space. According to the pull-off diagram, the solution predicts a 2.1σ higher Ar-production rate and 2.6σ lower SK rate, and no day-night asymmetry.

The SSM restricted global fit shifts the best fit point to an ''island'' centered around

$$\Delta m^2 = 4.8\times 10^{-10}\ \text{eV}^2, \qquad \tan^2\theta = 1.9. \tag{14}$$

Now $f_B = 0.72$. This solution was found by other groups too. The solution in the same ''island'' of the oscillation parameter space already appeared earlier (after 508 days of SK operation) when a significant excess of events in the high energy part of the spectrum was observed. The solution was later excluded by SK data on the spectrum. After the SNO result it reappeared again. The solution can reproduce a bump at $E\sim 8$ MeV and the increase of $R_{\nu e}$ at high energies.

Thus, in the VAC region there are three local minima (two of them are degenerate) with rather close χ^2. Small variations in the analysis shift the best fit VAC point from one minimum to another.

Although the VAC solution provides a very good fit to the data in the free flux global analysis, it does not pass additional criteria of quality. It requires very strong deviations of the boron and hep neutrino fluxes from the SSM values. The goodness of the fit becomes substantially worse when the SSM restrictions are imposed on these fluxes. There are significant deviations in the pull-off diagram.

The just-so^2 solution looks extremely unlikely in light of the SNO result. It gives a very poor fit to the rates. In fact, the fit is so bad that even the flat spectrum that it predicts, in agreement with the SK measurement, is not sufficient to make it plausible. Given the excellent fit of the LMA solution, the Just-So^2 solution is ruled out at 3σ C.L. This result is in agreement with Ref. [8]. Note that if the SNO experiment fails to observe a large day-night asymmetry, the situation might change, and the Just-So^2 solution might reappear at about $\sim 3\sigma$ C.L.

E. How large is large mixing?

This question is crucial for theory. In a number of approaches to bilarge mixing one gets mixing of the electron neutrino that is very close to maximal mixing (see [32] for a general discussion).

In the LMA region we find from the free flux analysis

$$\tan^2\theta < \begin{cases} 0.68, & 95\% \quad \text{C.L.}, \\ 0.82, & 99\% \quad \text{C.L.}, \\ 1.05, & 99.73\% \quad \text{C.L.}, \end{cases} \tag{15}$$

and, as we discussed in Sec III A, maximal mixing is allowed at $\sim 3\sigma$ level for $\Delta m^2 = (4-10)\times 10^{-5}$ eV^2. In the SSM restricted analysis the bounds become stronger.

In the LOW region we find $\tan^2\theta < 0.9$ at the 95% C.L. Maximal mixing is accepted at slightly lower than 99% C.L. in the range 6×10^{-9}–3×10^{-7} eV^2, which covers the LOW and the so-called QVO (quasivacuum oscillation) regions.

Maximal mixing is the best fit value of the Just-So^2 solution, although this solution is ruled out at the 3σ level in the global analysis. Notice that the fit of the data in the VAC region implies significant deviation from maximal mixing.

F. Do pure sterile solutions exist?

The best pure sterile solution (and the only one accepted at the 3σ level) is VAC(sterile), as could be expected from our pre-SNO analysis [5]. In the free flux analysis the solution already appears at the 90% C.L. with the best fit point:

$$\Delta m^2 = 1.4\times 10^{-10}\ \text{eV}^2, \qquad \tan^2\theta = 0.38(2.6),$$

$$f_B = 0.54, \qquad f_{\text{hep}} = 9. \tag{16}$$

Partially, the difference between the SK and SNO rates is explained by distortion of the spectrum: the suppression increases with increasing energy and therefore the higher threshold at SNO leads to lower averaged survival probability. However, mainly the fit ''shares'' the deviations between SNO and SK results: the solution requires a 1.2σ higher SNO rate and significantly lower boron neutrino flux, which gives a νe scattering rate 3.0σ below the SK result (see Fig. 3). The free flux analysis without the SK total rate does not locate this problem immediately. In principle, it should reappear in a fit of the spectrum with similar $\Delta\chi^2$ since the solution fits the shape of the spectrum rather well.

Notice that the parameters of this solution are very close to the parameters of VAC(active) apart from the two times larger hep flux. So this solution leads to the same type of spectrum distortion as the one described in Sec. III D with the bump at $E = 7$–8 MeV and the dip at $E = 11$–12 MeV.

In addition to a strong deviation of the νe scattering event rate from the SK result, the solution predicts a 2.1σ larger Ar-production rate. The fit worsens when SSM restrictions are imposed. For the SSM value of the hep neutrino flux the best fit point shifts to a smaller mixing angle and the χ^2 increases by $\Delta\chi^2 = 1.8$. In the analysis with the SSM restricted f_B, the goodness of the fit drops further: $\Delta\chi^2 = 6.2$. In the fit of the rates the solution shifts to smaller Δm^2 where the description of the SK spectra becomes bad. Thus, the solution does not pass additional quality tests.

The SMA(sterile) solution gives a very bad fit since it leads (in contrast with the VAC solution) to a distortion of the boron neutrino spectrum with suppression that weakens with increase of energy. This solution contradicts the SNO result: a 3.3σ higher rate is predicted.

Concerning sterile solutions one remark is in order. A better fit of the data can be obtained if more than one sterile neutrino participates in the conversion. Such a possibility is realized when solar neutrinos convert to the so called ''bulk'' neutrinos which propagate both in the usual and in (large) extra space dimensions [33]. From the four-dimensional point of view the solar ν_e is transformed to several Kaluza-Klein modes of the bulk neutrino, which show up as sterile

neutrinos. In this case one can reproduce (with low χ^2) the SK spectral data, and at the same time have better descriptions of the total rates (see [34] for a recent analysis).

IV. SNO: PREDICTIONS FOR THE NEXT STEP

Forthcoming results from SNO will include measurements of the day-night asymmetry and a more precise determination of the electron energy spectrum (higher statistics and lower energy threshold). Later, results on the NC/CC ratio will be available. Predictions for these observables have been extensively discussed before [35–40]. Here we sharpen the predictions using the latest solar neutrino data. We also calculate the expected values of the total event rate in the BOREXINO experiment which will start to operate soon.

A. Day-night asymmetry

We calculate the *D-N* asymmetry at SNO, A_{DN}^{SNO}, defined as

$$A_{DN}^{SNO} \equiv 2\frac{N-D}{N+D}, \tag{17}$$

for events above the threshold $E^{th}=6.75$ MeV.

We compare the asymmetry of the CC events at SNO with the asymmetry of the νe events measured at SK: A_{DN}^{SK}. There are three factors that can lead to substantially different SNO and SK asymmetries.

A "dumping" factor η_{dump} describes the suppression of the *D-N* asymmetry in the νe event rate due to the contribution of the ν_μ, ν_τ scattering to the signal. We get [16]

$$A_{DN}^{SNO} \propto \eta_{dump} A_{DN}^{SK}, \tag{18}$$

where

$$\eta_{dump} = 1 + \frac{r}{(1-r)\overline{P}}. \tag{19}$$

Here $r \equiv \sigma(\nu_\mu)/\sigma(\nu_e)$ is the ratio of cross sections of the $\nu_\mu e$ and $\nu_e e$ scattering, and $\overline{P}$ is the averaged survival probability. Notice that with decrease of $\overline{P}$ the damping factor increases.

A second factor η_{thr} describes the effect of difference of the energy thresholds: 5 MeV for SK and 6.75 MeV for SNO. It also accounts for the larger minimum difference (the binding energy of the deuteron, 1.44 MeV) between the neutrino energy and electron energy in the SNO experiment.

A third factor η_{reg} is related to the difference of the geographical latitudes. Since the Sudbury mine is at higher latitude, the regeneration effect there is slightly weaker than at Kamioka.

The total difference between the SNO and SK asymmetries is the product of these three factors.

Let us consider now the predictions for the asymmetries for individual solutions.

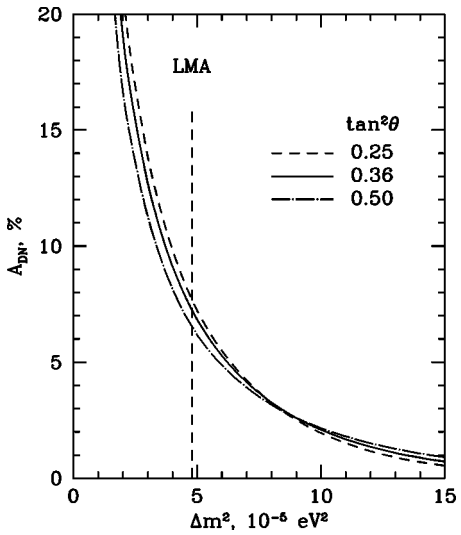

FIG. 4. The dependence of the day-night asymmetry of the CC-event rate measured at SNO on Δm^2 for different values of the mixing angle. The oscillation parameters are taken from the LMA allowed region. The best fit value of Δm^2 is marked by the vertical dashed line.

1. LMA solution

In Fig. 4 we show the dependence of the asymmetry on Δm^2 for different values of $\tan^2\theta$ from the allowed region. The asymmetry decreases with increase of Δm^2 as $\sim 1/\Delta m^2$ for $\Delta m^2 > 4\times 10^{-5}$ eV^2, and at larger Δm^2 the decrease is faster due to the effect of the adiabatic edge (see [17] for details). The dependence of the asymmetry on $\tan^2\theta$ is rather weak. At the best fit point we get

$$A_{DN}^{SNO} = 7.2\% \qquad (E^{th} = 6.75 \text{ MeV}). \tag{20}$$

In the allowed region the asymmetry can take any value from essentially zero to 15% at the 90% C.L. At the 3σ level it can reach 20%. The asymmetry is maximal at the smallest possible values of Δm^2 and $\tan^2\theta$ within the allowed region. It increases with the energy threshold due to increase of the regeneration factor: $f_{reg} \propto E/\Delta m^2$.

The expected asymmetry at SNO is substantially larger than at SK. At the best fit point we get $A_{DN}^{SK} = 3.6\%$; thus $A_{DN}^{SNO} \approx 2 \cdot A_{DN}^{SK}$. This difference can be easily understood by considering the factors mentioned above. Indeed, for the best fit point the survival probability can be estimated as $\overline{P} \approx R_{SNO}/f_B$. Inserting the numbers from Table V we get from Eq. (19) $\eta_{dump} = 1.6$. In the LMA region the asymmetry increases with increasing E_{th}. The threshold factor is $\eta_{thr} \sim 1.2$, and η_{reg} is close to 1. As a result, the overall enhancement factor at SNO is about 2.

2. LOW solution

The dependence of the asymmetry on Δm^2 for different values of $\tan^2\theta$ from the allowed region is shown in Fig. 5. At the best fit point (of the free flux analysis)

$$A_{DN}^{SNO} = 2.4\% \qquad (E^{th} = 6.75 \text{ MeV}). \tag{21}$$

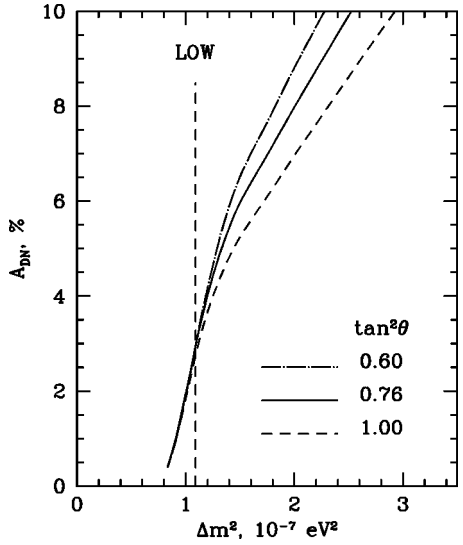

FIG. 5. The same as in Fig. 3(a) for the LOW solution. The dashed vertical line marks the best fit value of Δm^2 from the free flux fit.

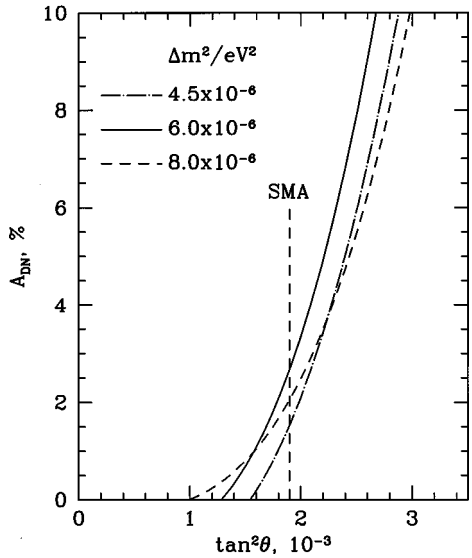

FIG. 6. The dependence of the day-night asymmetry of the CC-event rate measured at SNO on $\tan^2\theta$ for different values of Δm^2. The oscillation parameters are taken from the SMA allowed region. The best fit value of $\tan^2\theta$ is marked by the vertical dashed line.

The asymmetry increases linearly with Δm^2 for $\Delta m^2 > 10^{-7}$ eV^2. It can reach 10–12% at the upper border of the allowed (3σ) region. For $\Delta m^2 < 10^{-7}$ eV^2 the asymmetry decreases faster with deceasing Δm^2 due to the effect of the nonadiabatic edge (see [17] for details). It depends weakly on the mixing angle.

Let us emphasize that the *D-N* asymmetry at the best fit point of the LOW solution is substantially smaller than that in the LMA region. Thus, observation of an asymmetry $A_{DN}^{SNO} > 5\%$ will strongly favor the LMA solution.

In the LOW region the *D-N* asymmetry at SNO is also larger than in the SK detector. However, the difference here is not as large as in the LMA case. At the best fit point we get $A_{DN}^{SK} = 2\%$, which results in $A_{DN}^{SNO} = 1.2 A_{DN}^{SK}$. There are two reasons for this difference.

(i) The average survival probability is larger now (the mixing angle is larger): $\overline{P} \approx R_{SNO}/f_{\rm B} = 0.42$ (see Table V). As a consequence, the damping factor is smaller: $\eta_{damp} = 1.45$.

(ii) The difference in the thresholds works in the opposite direction in comparison with the LMA case, thus suppressing the SNO asymmetry. Indeed, in the LOW region the regeneration factor decreases with increasing $E/\Delta m^2$ and therefore the asymmetry decreases with increasing energy threshold. For $\eta_{thr} \sim 0.85$ we get a total enhancement factor in agreement with the exact calculation.

3. SMA solution

The dependence of the asymmetry on $\tan^2\theta$ for different values of Δm^2 is shown in Fig. 6. At the best fit point we get $A_{DN}^{SNO} = 2.6\%$ and most of this asymmetry is collected from the "core" bin. The asymmetry increases fast with $\tan^2\theta$. In the 3σ allowed region it can be as large as 8%.

The SNO asymmetry is only slightly higher than the SK asymmetry: $A_{DN}^{SK} = 2.4\%$. In the SMA range, due to strong dependence of the survival probability on energy, the relation between the SNO and SK asymmetries is more complicated than in Eq. (19).

B. Spectrum distortion

As follows from previous studies [39,40,31,41], in general the sensitivity of the SNO measurements to the energy spectrum distortion is higher than the sensitivity of SuperKamiokande due to better correlation of the neutrino and the (produced) electron energies. However, the present statistics at SNO is much lower than at SK, and the statistical errors are more than 2 times larger (in the range 8–10 MeV we get 10–12% at SNO as compared with 4–5% at SK).

In our analysis we do not use the spectral information from the SNO experiment. Instead, we present here a qualitative discussion comparing the present SNO data with predicted spectra from different solutions. This allows us to evaluate the significance of the present and forthcoming SNO results.

In Fig. 7 we show the expected spectra of events at SNO for several values of the oscillation parameters in the LMA region. In the high energy part of the spectrum the distortion is due to the earth regeneration effect as well as the contribution of the hep neutrino flux. However, for $\Delta m^2 \leqslant (4-5) \times 10^{-5}$ eV^2 the regeneration effect is small and the turnup at $E > 11$ MeV is due to increased ($f_{\rm hep} = 5$) flux of the hep neutrinos. The turnup of the spectrum at low energies is the effect of the adiabatic edge of the suppression pit. Recall that the ratio of the event rate with oscillations to the event rate with no oscillations is determined by the product of the survival probability times the factor $f_{\rm B}$: $R_{CC} \propto f_{\rm B}(\Delta m^2)\overline{P}(\Delta m^2)$. With increase of Δm^2 the spectrum shifts to the adiabatic edge; for $\Delta m^2 < 10^{-5}$ eV^2 the probability can be written as

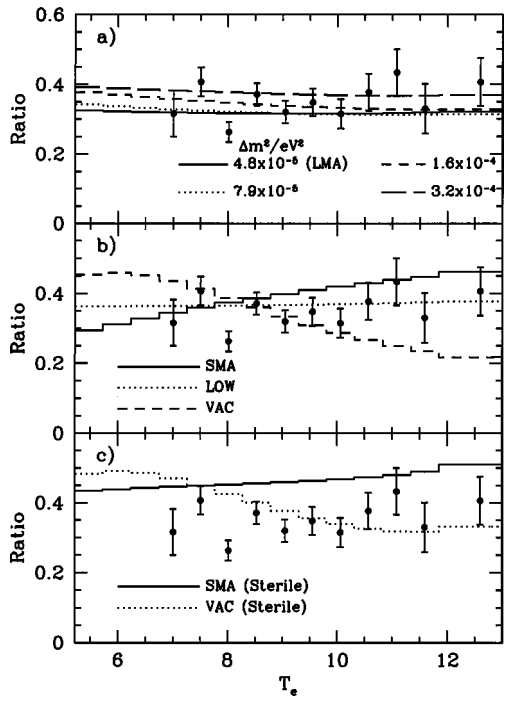

FIG. 7. The recoil electron energy spectra of the CC- events at SNO for global solutions of the solar neutrino problem. Shown are the ratios of the numbers of events with and without conversion as a function of the electron kinetic energy. (a) Spectra in the LMA solution region for different values of Δm^2 and $\tan^2\theta=0.35$. (b) Spectra for the best fit points of the SMA, LOW, and VAC(active) solutions. (c) Spectra for the best fit points of the SMA(sterile) and VAC(sterile) solutions. Shown also in all panels are the SNO experimental data.

$$\overline{P}\approx(\sin^2\theta+f_{reg}+A),$$

where A is the correction due to the adiabatic edge and is proportional to the first moment δT:

$$A\propto\delta T\propto\cos 2\theta\left(\frac{\Delta m^2}{E}\right)^2 \tag{22}$$

(see the Appendix of [17] for more details). The factor $\cos 2\theta$ accounts for the disappearance of the distortion when the mixing approaches its maximal value. With increasing Δm^2 the size of the turnup and the distortion of the spectrum (first moment) increase as $(\Delta m^2)^2$. Notice that at the same time $f_{\rm B}$ decreases to compensate for a total increase of the survival probability. The distortion reaches a maximum at $\Delta m^2 \sim 1.5\times10^{-4}$ eV^2 when the boron neutrino spectrum is in the middle of the adiabatic edge. With further increase of Δm^2, the spectrum shifts out of the suppression pit and the distortion decreases. For $\Delta m^2>3\times10^{-4}$ eV^2 the spectrum is in the range where the probability is determined basically by the averaged vacuum oscillations, $P=1-\sin^2 2\theta/2$, and does not depend on the neutrino energy. Notice that the distortion of the spectrum weakens due to integration over the neutrino energy and folding with the energy resolution function. Moreover, the SNO sensitivity to the distortion at low energies is weakened by the fast decrease of the cross section with increasing energy.

The curves shown in Fig. 7(a) illustrate this behavior of the spectrum. The short dashed line corresponds to near maximal distortion. As follows from the figure it will be very difficult to establish the distortion expected from the LMA solution with SNO data. One needs to measure the spectrum down to ~5 MeV and to increase the statistics substantially. Thus, the prediction for SNO is that no significant distortion should be seen in forthcoming measurements.

In Fig. 7(b) we show the expected spectra of events at SNO at the best fit points of the LOW, SMA, and VAC(active) solutions. The correlated systematic errors (mainly due to the error in the absolute energy scale calibration) are not shown here. These errors can affect the conclusions from the fit to the spectrum, making the spectrum appear flatter.

At the best fit point of the LOW solution the earth regeneration effect on the shape of the spectrum is small. The weak positive slope (positive shift of the first moment) is due to the effect of the adiabaticity violation (nonadiabatic edge of the suppression pit). The slope increases with decreasing $\tan^2\theta$ as well as Δm^2 (for some analytical studies see [17]). It will be difficult to establish this distortion with SNO data.

For the VAC(active) solution with low Δm^2, Eq. (13), a one predicts maximum of the ratio R_{CC} at $E\sim6$ MeV. It corresponds to the first oscillation maximum of the survival probability. The ratio decreases with increase of energy and at $E>11$ MeV the distortion flattens due to the contribution of the hep neutrino flux. Thus, a negative shift of the first moment (slope) is expected. As follows from the figure, the distortion is at the border of sensitivity of already present SNO data (correlated systematic errors can somewhat improve the agreement between the data and the predictions). A further increase of statistics and especially measurements of the spectrum at lower energies will be crucial for discrimination of the solution. Notice that the oscillation parameters are well fixed by the SK spectrum, and no freedom exists, e.g., to change the distortion by varying Δm^2. In particular, the position of the maximum at $E\sim6$ MeV is immediately determined by the maximum in the SK spectrum at 8 MeV. The distortion can be identified by comparison of the averaged ratio R_{CC} at low and high energies: $R_{CC}(<9$ MeV) and $R_{CC}(>9$ MeV).

A similar distortion is expected for the VAC(sterile) solution; see Fig. 7(c). For VAC(active) with high Δm^2 [see Eq. (14)] one expects a flat distribution at low energies due to a strong averaging effect and a bump at high energies $E>12$ MeV.

For the SMA(active) solution there is a strong positive shift of the first moment (slope). Correlated systematic errors improve the agreement with the experimental data. The present SNO data can already have some impact on this solution. The allowed region will drift to smaller mixing angles where the distortion is weaker. The best fit boron flux should decrease in order to compensate for the increase of the survival probability.

For the SMA(sterile) solution the distortion is very weak, as a consequence of very small mixing angle. However, for

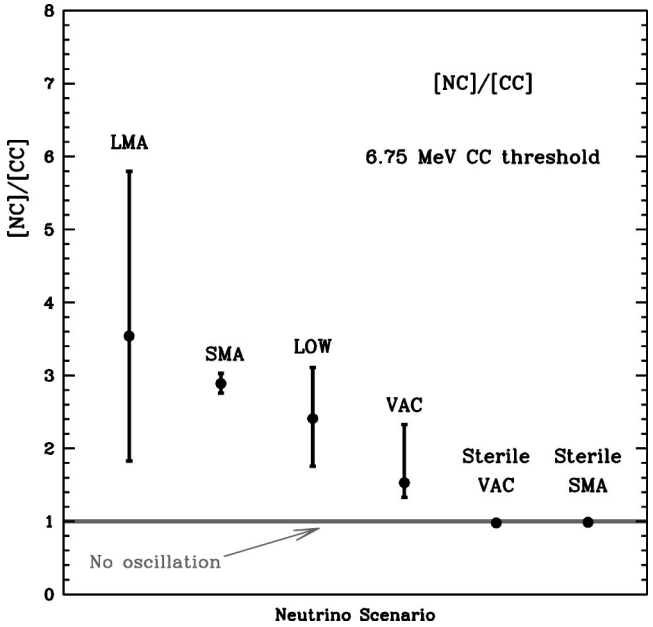

FIG. 8. The ratio of the reduced NC event rate to the reduced CC event rate. The circles give values of [NC]/[CC] at the best fit points of the global solutions. The error bars show the prediction intervals of [NC]/[CC] that correspond to the 3σ allowed regions of global solutions.

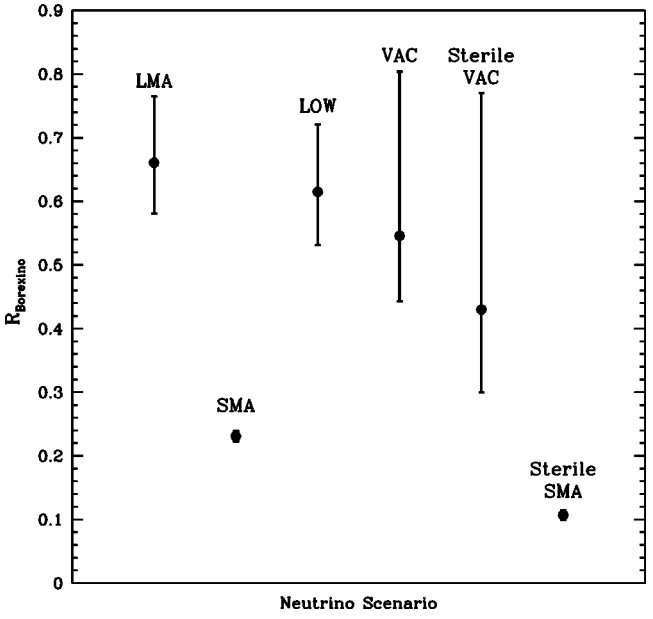

FIG. 9. The reduced event rate in the BOREXINO experiment. The circles give values of $R_{BOREXINO}$ at the best fit points of the global solutions. The error bars show the prediction intervals that correspond to the 3σ allowed regions of the global solutions.

this solution the predicted spectrum is systematically above the experimental points, which corresponds to a 3.3σ higher total rate.

In conclusion, the present SNO spectral data further favor the LMA and LOW solutions. However, it will be difficult to establish with the SNO data the weak spectral distortions expected for these solutions. At the same time, the SNO measurements can be sensitive to the strong distortion of the spectrum predicted by already disfavored solutions such as VAC and SMA.

C. NC/CC ratio

The reduced neutral current event rate [NC] is defined as the ratio of the rates with and without oscillations: $[\mathrm{NC}] \equiv N_{NC}/N_{NC}^{SSM}$. Similarly, the reduced rate of the charged current event rate $[\mathrm{CC}] \equiv N_{CC}/N_{CC}^{SSM}$. We have calculated the ratio of the NC and CC reduced rates, [NC]/[CC], for global solutions found from the free flux fit.

For the active neutrino conversion the ratio equals

$$\frac{\mathrm{NC}}{\mathrm{CC}} = \frac{1}{\overline{P}} \approx \frac{f_{\mathrm{B}}}{R_{SNO}}, \tag{23}$$

where $\overline{P}$ is the effective (averaged) survival probability of the electron neutrinos. At the best fit points, using results for f_{B} and R_{SNO} from Tables I and V, we find [NC]/[CC] $=3.5$ (LMA), 2.4 (LOW), 2.8 (SMA), 1.5 (VAC), and ≈ 1 (Just-So^2) in agreement with the results of numerical calculations (see Fig. 8).

For the sterile solutions we have

$$\frac{[\mathrm{NC}]}{[\mathrm{CC}]} = \frac{\overline{P}_{NC}}{\overline{P}_{CC}}, \tag{24}$$

where $\overline{P}_{NC}$ and $\overline{P}_{CC}$ are the effective survival probabilities for the NC and CC samples, respectively. For the NC sample the energy threshold is about 2.2 MeV, so that P_{NC} is averaged over a larger interval than P_{CC}. As a consequence, the probabilities $\overline{P}_{CC}$ and $\overline{P}_{NC}$ are different in general.

Notice that the largest value of the ratio is expected for the LMA solution:

$$\frac{[\mathrm{NC}]}{[\mathrm{CC}]} = 3.5^{+2.4}_{-1.7} \qquad (\mathrm{LMA}). \tag{25}$$

Then rather close predictions follow from the SMA and LOW solutions. A smaller value is predicted for the VAC solution. For sterile solutions the ratio is close to 1.

According to Fig. 8, there is a significant overlap of the 3σ regions of predictions. However, measurements of the ratio with better than 20% accuracy can significantly contribute to discrimination of the solutions.

D. BOREXINO rate

For global solutions we have calculated the reduced event rate in the BOREXINO experiment [42], $R_{BOREXINO} \equiv N_{osc}/N_{SSM}$, where N_{osc} and N_{SSM} are the expected rates with and without neutrino conversion. We averaged the effect over the year.

The rate can be estimated as $R_{BOREXINO} = \overline{P}_{\mathrm{Be}}(1-r)+r$, where $\overline{P}_{\mathrm{Be}}$ is the averaged survival probability for the ^{7}Be neutrino line. The probability $\overline{P}_{\mathrm{Be}}$ has been calculated for the

oscillation parameters from the 3σ allowed regions of solutions found from the free flux analysis. r is the ratio of cross sections of the $\nu_\mu e$ and $\nu_e e$ scattering at the the beryllium line. We have used the neutrino-electron scattering cross sections from Ref. [43].

The results of calculations for six global solutions are shown in Fig. 9. The rate is suppressed for all solutions. In particular, for the LMA solution we get

$$R_{BOREXINO} = 0.66^{+0.11}_{-0.08} \qquad \text{(LMA)}.$$

A similar suppression is expected for the LOW solution. The VAC solutions predict stronger suppression and the lowest rate is expected for the SMA. Notice that the range of predictions for the SMA solution is very small due to the smallness of the allowed region itself.

There is a significant overlap of the predicted intervals for LMA, LOW, and VAC solutions. Therefore, it will be difficult to discriminate among these solutions using just total rate measurements. However, BOREXINO has other capabilities, e.g., it can detect a strong day-night effect in the case of the LOW solutions [44], whereas strong seasonal variations are expected if either the QVO or VAC solution is realized [45].

V. CONCLUSIONS

We have performed a global analysis of the solar neutrino data including the charged current event rate measured by the SNO experiment. We tested the robustness of the global solutions by modifying the analysis. The quality of the fit was checked by construction of the pull-off diagrams.

We find that the LMA solution with parameters in the range $\Delta m^2 \sim (4\text{–}5)\times 10^{-5}$ eV^2 and $\tan^2\theta = 0.35\text{–}0.40$ gives the best fit to the data. Moreover, the solution reproduces the flat spectrum of recoil electrons at SK and gives a very good description of the rates and of the day-night asymmetry. It is in very good agreement with the SSM fluxes of the boron ($f_{\rm B} = 1.10\text{–}1.13$) and hep neutrinos. The values of the oscillation parameters and the goodness of the fit are stable with respect to variations of the analysis.

The LOW solution appears at 90% C.L. with respect to the best fit point in the LMA range. It gives a good fit to the SK spectral data, but a rather poor fit to the rates: it predicts a larger than measured Ar-production rate and a smaller than measured Ge-production rate.

The VAC solution has a high goodness of global fit due to a very good description of the day and night spectra measured by the SK experiment. It has problems with other criteria, however. The solution requires strong deviation of the boron and hep fluxes from their SSM values. The fit becomes substantially worse when SSM restrictions are applied. The solution shows strong deviations in the pull-off diagram (especially for the SuperKamiokande rate and the Ar-production rate). The analysis of the rates only selects a different point in the oscillation parameter space.

The SMA solution appears at about 3σ C.L. level with respect to the best global solution in the LMA range. It gives a bad fit of the recoil electron energy spectrum and also the fit of the rates is rather poor.

The best sterile solution is VAC(sterile) with $\Delta m^2 = 1.4 \times 10^{-10}$ eV^2. It is the only sterile solution accepted at lower than 3σ C.L. in the free flux analysis. This solution, however, has serious problems with other tests. Similarly to VAC(active), the solution requires strong deviation of the boron and hep fluxes from their SSM values. The fit becomes substantially worse when SSM restrictions are applied. The solution shows strong deviations in the pull-off diagram: in particular, the νe event rate is about 3σ below the SK rate, and the Ar-production rate is 2.4σ higher than the Homestake result. The analysis of the rate only selects a different point in the oscillation parameter space. Significant distortion of the energy spectrum is expected. The appearance of the VAC solutions (both active and sterile) in the global fit is related to a small spread of the experimental points in the SK spectrum. These solutions can describe rather precisely the bump at 7–8 MeV and the dip at 11–12 MeV.

Maximal mixing is allowed at the 3σ level in the LMA region and at the 99% C.L. in the LOW and quasivacuum oscillation regions.

Measurements of the D-N asymmetry will provide strong discrimination among the solutions. In the best fit range of the LMA solution the asymmetry at SNO is $A_{DN}^{SNO} \simeq 7\text{–}8\,\%$, and in the 3σ allowed region it can reach 15–20 %. In the LOW region one expects smaller asymmetry: at the best fit point $A_{DN}^{SNO} \simeq 2\text{–}3\,\%$, although in the 3σ allowed region it can be as large as 10–12 %. For the SMA solution the asymmetry is $A_{DN}^{SNO} \leqslant 3\%$. The predicted SMA zenith angle distribution is not supported by SK data.

Clearly, observation of a large D-N asymmetry $A_{DN}^{SNO} > 5\%$ will favor the LMA solution. It will strongly disfavor the SMA solution, and exclude solutions based on vacuum oscillations (VAC, QVO, and Just-So^2). Furthermore, this result will strongly restrict the LMA solution to lower Δm^2. Even with existing statistics (the expected error is $3-4\,\%$)any SNO result on the D-N asymmetry will be of physical importance, excluding some solutions or further restricting the allowed regions.

Significant distortion of the boron neutrino spectrum is expected for SMA and VAC solutions and already the present data can affect them. The VAC solution predicts the bump at 6 MeV and the dip at 11 MeV in the dependence of the R_{CC} on energy. In the case of the LMA solution a turnup of the spectrum at low energies is expected, which will be rather difficult to observe at SNO. For the LMA and LOW solutions one expects essentially no distortion in future SNO measurements.

Important discrimination among solutions can be done using a precise determination of the [NC]/[CC] ratio. If the soon-to-be-measured value of the [NC]/[CC] ratio turns out to be significantly different from 1 it will become further important evidence for neutrino oscillations. The value of the measured ratio can also help distinguish between competing solutions which presently provide comparable fits to the solar neutrino data.

Additional information about the oscillation hypothesis is

expected to come from the KamLAND reactor experiment [46]. According to Ref. [47], if the LMA solution is the correct one, KamLAND will be able to determine the oscillation parameters with high accuracy. Recently it was pointed out in Ref. [48] that the complications arising in the large ($\Delta m^2 > 10^{-4}$ eV^2) part of the LMA solution, for which KamLAND will not be able to see a clear oscillation signal, can be resolved with intermediate long baseline (≈ 20 km) reactor experiments.

The forthcoming SNO data will undoubtedly provide important empirical information and might become the next major step in identifying the solution of the solar neutrino problem.

ACKNOWLEDGMENTS

The authors are grateful to J. Beacom, E. Lisi, and M. C. Gonzalez-Garcia for comments on the first version of the paper. We thank Y. Suzuki for clarification of the way the SuperKamiokande Collaboration treat the hep neutrino flux in the analysis of the data. This work was supported by DGICYT under grant PB95-1077 and by the TMR network grant ERBFMRXCT960090 of the European Union. The calculations were performed on the computers at the Institute for Advanced Study in Princeton and the Nuclear Astrophysics Group at the Department of Physics and Astronomy, UW-Madison. Support for the calculations was provided under NSF grants No. PHY0070928 and No. PHY0070161.

[1] SNO Collaboration, Q.R. Ahmad *et al.*, Phys. Rev. Lett. **87**, 071301 (2001)

[2] A.B. McDonald, in *Neutrino 2000*, Proceedings of the International Conference on Neutrino Physics and Astrophysics, Neutrino 2000, Sudbury, Canada, 2000, Nucl. Phys. B (Proc. Suppl.) **91**, 21 (2001).

[3] SuperKamiokande Collaboration, S. Fukuda *et al.*, Phys. Rev. Lett. **86**, 5651 (2001).

[4] J.N. Bahcall, Phys. Rev. C **65**, 015802 (2002); **65**, 025801 (2002); V. Berezinsky, hep-ph/0108166.

[5] J.N. Bahcall, P.I. Krastev, and A.Yu. Smirnov, J. High Energy Phys. **05**, 15 (2001).

[6] See previous analyses of this type: Waikwok Kwong and S.P. Rosen, Phys. Rev. D **54**, 2043 (1996); F.L. Villante, G. Fiorentini, and E. Lisi, *ibid.* **59**, 013006 (1999); J.N. Bahcall, P.I. Krastev, and A.Yu. Smirnov, Phys. Lett. B **477**, 401 (2000).

[7] V. Barger, D. Marfatia, and K. Whisnant, Phys. Rev. Lett. **88**, 011302 (2002).

[8] G.L. Fogli, E. Lisi, D. Montanino, and A. Palazzo, Phys. Rev. D **64**, 093007 (2001).

[9] J.N. Bahcall, M.C. Gonzalez-Garcia, and Carlos Pena-Garay, J. High Energy Phys. **08**, 014 (2001).

[10] A. Bandyopadhyay, S. Choubey, S. Goswami, and K. Kar, Phys. Lett. B **519**, 83 (2001).

[11] A. de Gouvea and C. Pena-Garay, Phys. Rev. D **64**, 113011 (2001).

[12] R. Barbieri and A. Strumia, J. High Energy Phys. **12**, 016 (2000).

[13] C. Giunti, Phys. Rev. D **65**, 033006 (2002).

[14] V. Berezinsky and M. Lissia, Phys. Lett. B **521**, 287 (2001).

[15] J.N. Bahcall, P.I. Krastev, and A.Yu. Smirnov, Phys. Rev. D **58**, 096016 (1998).

[16] J.N. Bahcall, P.I. Krastev, and A.Yu. Smirnov, Phys. Rev. D **62**, 093004 (2000).

[17] J.N. Bahcall, P.I. Krastev, and A.Yu. Smirnov, Phys. Rev. D **63**, 053012 (2001).

[18] B.T. Cleveland *et al.*, Astrophys. J. **496**, 505 (1998); K. Lande *et al.*, in *Neutrino 2000* [2], p. 50.

[19] SAGE Collaboration, V. Gavrin, in *Neutrino 2000* [2], p. 36.

[20] GALLEX Collaboration, W. Hampel *et al.*, Phys. Lett. B **447**, 127 (1999).

[21] GNO Collaboration, M. Altmann *et al.*, Phys. Lett. B **490**, 16 (2000); E. Bellotti *et al.*, in *Neutrino 2000*, [2], p. 44.

[22] J.N. Bahcall, M.H. Pinsonneault, and S. Basu, Astrophys. J. **555**, 990 (2001).

[23] P.I. Krastev and A.Yu. Smirnov, Phys. Lett. B **338**, 282 (1994).

[24] L.E. Marcucci *et al.*, Phys. Rev. C **63**, 015801 (2001); T.-S. Park *et al.*, nucl-/0107012, and references therein.

[25] P. Creminelli, G. Signorelli, and A. Strumia, J. High Energy Phys. **05**, 052 (2001).

[26] J.N. Bahcall, P.I. Krastev, and A.Yu. Smirnov, Phys. Rev. D **60**, 093001 (1999).

[27] S. Geer, Phys. Rev. D **57**, 6989 (1998).

[28] CHOOZ Collaboration, M. Apollonio *et al.*, Phys. Lett. B **420**, 397 (1998).

[29] S. P. Mikheyev and A. Yu. Smirnov, in *'86 Massive Neutrinos in Astrophysics and in Particle Physics*, Proceedings of the 6th Moriond Workshop, edited by O. Fackler and J. Tran Thanh Van (Edition Frontiers, Gif-sur-Yvette, 1986), p. 355; A.J. Baltz and J. Weneser, Phys. Rev. D **50**, 5971 (1994); **51**, 3960 (1994); E. Lisi and D. Montanino, *ibid.* **56**, 1792 (1997); J.M. Gelb, Wai-kwok Kwong, and S.P. Rosen, Phys. Rev. Lett. **78**, 2296 (1997).

[30] S.T. Petcov, Phys. Lett. B **434**, 321 (1998); E.Kh. Akhmedov, Nucl. Phys. **B538**, 25 (1999); M.V. Chizhov and S.T. Petcov, Phys. Rev. Lett. **83**, 1096 (1999).

[31] K.S. Babu, Q.Y. Liu, and A.Yu. Smirnov, Phys. Rev. D **57**, 5825 (1998).

[32] M.C. Gonzalez-Garcia, C. Pena-Garay, Y. Nir, and A.Yu. Smirnov, Phys. Rev. D **63**, 013007 (2001).

[33] G. Dvali and A.Yu. Smirnov, Nucl. Phys. **B563**, 63 (1999).

[34] A. Lukas, P. Ramond, A. Romanino, and G.G. Ross, J. High Energy Phys. **04**, 010 (2001); D.O. Caldwell, R.N. Mohapatra, and S.J. Yellin, Phys. Rev. D **64**, 073001 (2001).

[35] J.N. Bahcall and P.I. Krastev, Phys. Rev. C **56**, 2839 (1997).

[36] M. Maris and S.T. Petcov, Phys. Rev. D **62**, 093006 (2000).

[37] G.L. Fogli, E. Lisi, D. Montanino, and A. Palazzo, Phys. Rev. D **62**, 113003 (2000).

[38] M.C. Gonzalez-Garcia, C. Pena-Garay, and A.Yu. Smirnov, Phys. Rev. D **63**, 113004 (2001).

[39] J.N. Bahcall and E. Lisi, Phys. Rev. D **54**, 5417 (1996).

[40] J.N. Bahcall, P.I. Krastev, and E. Lisi, Phys. Rev. C **55**, 494 (1997).

[41] G.L. Fogli, E. Lisi, and D. Montanino, Astropart. Phys. **9**, 119 (1998).
[42] BOREXINO Collaboration, G. Ranucci *et al.*, in *Neutrino 2000* [2], p. 58.
[43] J.N. Bahcall, M. Kamionkowski, and A. Sirlin, Phys. Rev. D **51**, 6146 (1995).
[44] A.J. Baltz, and J. Weneser, Phys. Rev. D **50**, 5971 (1994); **51**, 3960 (1995); for a recent analysis, see A. de Gouvea, A. Friedland, and H. Murayama, J. High Energy Phys. **03**, 009 (2001); G.L. Fogli, E. Lisi, D. Montanino, and A. Palazzo, Phys. Rev. D **61**, 073009 (2000).
[45] For a recent analysis, see B. Faid, G.L. Fogli, E. Lisi, and D. Montanino, Astropart. Phys. **10**, 93 (1999); A. de Gouvea, A. Friedland, and H. Murayama, Phys. Rev. D **60**, 093011 (1999).
[46] KamLAND Collaboration, A. Piepke, Nucl. Phys. B (Proc. Suppl.) **91**, 99 (2001).
[47] V. Barger, D. Marfatia, and B.P. Wood, Phys. Lett. B **498**, 53 (2001); R. Barbieri and A. Strumia, J. High Energy Phys. **12**, 016 (2000).
[48] S.T. Petcov and M. Piai, hep-ph/0112074.